

Molecular hydrodynamic theory of the velocity autocorrelation function

S. L. Seyler^{1, a)} and C. E. Seyler²

¹⁾*School of Molecular Sciences, Arizona State University, Tempe, AZ 85287*

²⁾*Laboratory of Plasma Studies, Cornell University, Ithaca, NY 14853*

(Dated: April 4, 2023)

The velocity autocorrelation function (VACF) encapsulates extensive information about the molecular-structural and hydrodynamic properties of a fluid. We address the following fundamental question: How well can a purely hydrodynamic model recover the molecular properties of a fluid as exhibited by the VACF? To this end, we develop a bona fide hydrodynamic theory of the tagged-particle VACF for simple fluids. Our approach is distinguished from previous efforts in two key ways: collective hydrodynamic modes are described by *linear* hydrodynamic equations obtained as velocity moments of a single-particle kinetic equation; the fluid's static kinetic energy spectrum is identified as a necessary initial condition for the momentum current correlation. This leads to a natural physical interpretation of the molecular-hydrodynamic VACF as a superposition of quasinormal hydrodynamic modes weighted commensurately with the static kinetic energy spectrum. Our method yields VACF calculations quantitatively on par with existing approaches for liquid noble gases and alkali metals; moreover, our hydrodynamic formulation of the self-intermediate scattering function appears to extend the description to low densities where the Schmidt number is of order unity, enabling calculations for the vapor and supercritical phases.

INTRODUCTION

The velocity autocorrelation function (VACF) is, perhaps, the quintessential time-correlation function, as it holds unique significance in condensed matter physics and chemistry.^{1–3} In particular, the VACF is intrinsically linked to Brownian motion: the self-diffusion coefficient, D_s , of a large diffusing particle is the time integral of the VACF, a connection traceable to the famous Einstein relation, $D_s = \lim_{t \rightarrow \infty} \langle |\mathbf{x}(t) - \mathbf{x}(0)|^2 \rangle / 6t$.⁴ It was therefore unexpected when Alder and Wainwright,^{5,6} using molecular dynamics (MD) simulations, revealed that the VACF of a “tagged” fluid particle—one mechanically identical to all others—decays as $t^{-3/2}$ at long times, not exponentially as predicted by Chapman-Enskog-Boltzmann theory.^{7–11} Using simple physical arguments, they recognized that this protracted decay was due to delayed viscous momentum transport—a phenomenon known as *hydrodynamic memory*.

Zwanzig and Bixon¹² promptly recognized that a viscoelastic hydrodynamic VACF formulation could account for both slow hydrodynamic decay and molecular-scale fluid granularity. Although Zwanzig-Bixon theory remains questionable at short times, its success for liquid argon substantiates the hydrodynamic perspective.^{1,13} The fluid particle VACF, which probes fluid structure and dynamics across all timescales, has broad utility, but efforts to obtain physically consistent analytic models spanning all space-time scales and densities have been hampered by subtle challenges.^{14–17} Meanwhile, MD simulation, along with techniques driven by the memory function and projection operator formalisms,^{18–20} has been a workhorse for probing kinetic aspects of

fluids,^{21–32} as well as furnishing coarse-graining (CG) techniques for multiscale modeling.^{33–38}

Nevertheless, the mesoscopic nature of complex fluid systems, including nanocolloidal suspensions,^{39–41} microswimmers,^{42–44} solvated biomolecules,^{45–48} and others,^{49–52} involves long-ranged hydrodynamic interactions, as well as passive and active Brownian motion, which poses substantial challenges to particle-based numerical simulation. And yet, it is not clear for even simple fluids³ what general rules delineate the applicable domain of continuum hydrodynamic models, especially near molecular scales.^{30,53} What are the smallest space-time scales down to which a hydrodynamic model can yield a viable theory of the VACF? And, more generally, what ingredients are necessary to bridge continuum and discrete-particle behavior at molecular scales?

In this Communication, we formulate a theory of the VACF from a purely hydrodynamic standpoint that directly confronts these questions. Central to our framework is a general set of physical *desiderata* (Table I), which constrains a chosen hydrodynamic model so as to correctly reproduce both short-time molecular kinetics and collective dynamics across all timescales while minimizing ad hoc assumptions. Crucially, we find physical consistency requires that the equal-time velocity covariance be an integrable distribution over wavenumber, which we identify as an initial condition corresponding to the fluid's static kinetic energy spectrum. These considerations lead to a general theory that represents a considerably different physical picture than the otherwise formally similar velocity-field approach.^{13,54–58}

To this end, we develop a 10-moment molecular-hydrodynamic model based on the well-established 13-moment equations,^{59–66} which originate as velocity moments of the linearized BGK-Boltzmann kinetic equation.^{67–69} The resulting moment-equations naturally lead to wavenumber-dependent current correlations

^{a)}Electronic mail: slseyler@asu.edu

Table I. Desiderata and constraints for physically admissible correlation functions.

Desideratum (req.)	Expression	Remarks
(1) memory equation ^a	$\dot{C} + \int_0^t d\tau K(k, t-\tau) C(k, \tau) = 0$	Memory kernel $K(k, t)$ must be consistent with desiderata.
(2) normalizability ^a	$C(k, 0) = 1$	Static spectrum must be integrable: $\int_0^\infty dk k^2 q(ka)$ exists.
(3) time reversibility ^a	$\dot{C}(k, 0) = 0$	Process must be time-reversal symmetric.
(4) exponential range ^a	$C_\perp(k, t) \sim e^{-t/\tau_\perp}, F_s(k, t) \sim e^{-t/\tau_s}$	Must decay exponentially for $kv_0 > \tau_{\perp,s}^{-1}$ at lower densities. ^c
(5) ballistic range ^{ab}	$\psi(t) \sim \mathcal{N} \int_0^\infty dk k^2 q(ka) e^{-k^2 v^2 t^2/2}$	Short-time sum rule constrains a using ω_E for liquids. ^d
(6) diffusive range ^{ab}	$C_\perp(k, t) F_s(k, t) \sim e^{-k^2(\nu + D_s)t}$	Must preserve long-time asymptotic form of VACF. ^e
(7) long-time diffusivity ^b	$D_s = \mathcal{N} \int_0^\infty dt \int_0^\infty dk k^2 q(ka) C_\perp(k, t) F_s(k, t)$	Zero-frequency sum rule from Green-Kubo relation. ^f

^aGeneral requirements that constrain the functional forms of correlation functions.

^bSpecific requirements that constrain the values of correlation function parameters.

^cRequires $\mathcal{D}_\perp, D_s \neq 0$ and k -independence of C_\perp and F_s for large k . See Appendix D.

^dSum rule constraint is valid when Einstein frequency, ω_E , is well defined, e.g. for liquids. See Appendix B.

^eImplies the invariant forms $a^2 v$ and $a^2 \gamma_s$. See Eqs. (32) to (33) and Eqs. (D6) and (D7).

^fLiquids: $C_\parallel \approx 0, F_s \approx 1$ yields analytic solution for \mathcal{D}_\perp . Gases: $C_\parallel \approx 0$ yields constraint for $\gamma_s, \mathcal{D}_\perp$. See Appendices C and D.

that reproduce, among other phenomena, molecular-scale viscoelasticity.^{70,71} As a point of contrast, *generalized hydrodynamics*^{1,3,72} begins with the Navier-Stokes equations, extending them to molecular scales by phenomenologically promoting transport coefficients to nonlocal quantities with frequency- and wavenumber-dependence. In practice, the velocity-field approach leverages generalized hydrodynamics and has been used with notable success.^{72–80}

The present theory offers important advantages, however. In particular, it implies a natural physical interpretation of the hydrodynamic VACF: a superposition of quasinormal hydrodynamic modes, each mode k having a wavelength $2\pi/k$ and weight $\langle u_k^2 \rangle$ proportional to the equilibrium probability density of fluid kinetic energy. Moreover, unlike other approaches, the methodology enables realistic VACF calculations not only for simple liquids, but also *gases* using the same underlying framework. We apply the methodology to representative fluids—liquid rubidium and argon, and gaseous and supercritical argon—and find remarkable agreement with MD calculations.^{24,28,32,81}

THEORY OF THE HYDRODYNAMIC VACF

Let $\mathbf{u}(\mathbf{x}, t)$ be the Eulerian velocity field of a fluid derived as the velocity moment of an exact single-particle distribution function, $f(\mathbf{x}, \mathbf{v}, t)$, and $\mathbf{x}_\alpha(t)$ be the position of constituent particle α of mass m . We then require the fluid velocity at $\mathbf{x}_\alpha(t)$ to be equal to the particle velocity: $\mathbf{u}[\mathbf{x}_\alpha(t), t] = \mathbf{v}_\alpha(t)$, where $\mathbf{v}_\alpha(t) \equiv \dot{\mathbf{x}}_\alpha(t)$. Expressing the Lagrangian velocity using Fourier components $\mathbf{u}_\mathbf{k}(t)$,

$$\mathbf{u}[\mathbf{x}_\alpha(t), t] = \int dk \mathbf{u}_\mathbf{k}(t) e^{i\mathbf{k} \cdot \mathbf{x}_\alpha(t)} \quad (1)$$

the velocity covariance $Q(t) \equiv \langle \mathbf{v}_\alpha(0) \cdot \mathbf{v}_\alpha(t) \rangle$ becomes

$$Q(t) = \langle \mathbf{u}[\mathbf{x}_\alpha(0), 0] \cdot \mathbf{u}[\mathbf{x}_\alpha(t), t] \rangle$$

$$= \int dk dk' \langle \mathbf{u}_\mathbf{k}(0) \cdot \mathbf{u}_\mathbf{k}'(t) e^{i\mathbf{k} \cdot \mathbf{x}_\alpha(0) + i\mathbf{k}' \cdot \mathbf{x}_\alpha(t)} \rangle \\ \approx \int dk \langle \mathbf{u}_\mathbf{k}^*(0) \cdot \mathbf{u}_\mathbf{k}(t) \rangle \langle e^{i\mathbf{k} \cdot [\mathbf{x}_\alpha(t) - \mathbf{x}_\alpha(0)]} \rangle \quad (2)$$

where in the last line we assume a spatially homogeneous system and decompose the ensemble average into a product of averages. Importantly, we assume *a priori* uncorrelated particle displacements and fluid velocities whose underlying correlations will be reproduced by applying appropriate physical constraints (cf. Table I).

Assuming an isotropic fluid, we decompose the modal velocity covariance, $Q(k, t) \equiv \langle \mathbf{u}_\mathbf{k}^*(0) \cdot \mathbf{u}_\mathbf{k}(t) \rangle = q(k) C(k, t)$, where $q(k) \equiv Q(k, 0)$ and $C(k, t) = Q(k, t)/q(k)$ is the (normalized) current correlation; the characteristic function for tagged-particle displacements is the self-intermediate scattering function (SISF), $F_s(k, t) \equiv \langle \exp\{i\mathbf{k} \cdot [\mathbf{x}_\alpha(t) - \mathbf{x}_\alpha(0)]\} \rangle$. Altogether, this yields a general expression for the VACF

$$\psi(t) = \mathcal{N} \int_0^\infty dk k^2 q(k) C(k, t) F_s(k, t) \quad (3)$$

where $\mathcal{N} \equiv [\int_0^\infty dk k^2 q(k)]^{-1}$ is the normalization at $t = 0$.

Equilibrium energy partitioning

From Eq. (3), it is apparent that the customary statement of equipartition, $q(k) = k_B T/m$, leads to a divergent integral. This is unsurprising, as a true white noise spectrum is unphysical. Thus, the fluid static kinetic energy spectrum, or *spectral density* for short,

$$q(k) \equiv \langle |u_k(0)|^2 \rangle \quad (4)$$

must contain a microscopic parameter, a , that attenuates large-wavenumber contributions. In turbulence theory, a

fundamental quantity analogous to $q(k)$ is the omnidirectional kinetic energy spectrum, $E(k) = 2\pi\rho k^2 q(k)$.⁸²⁻⁸⁴

The inverse Fourier transform of $q(k)$ is formally identical to the “form factor,” $f(r)$, in the velocity-field method, wherein a is *a priori* treated as an effective molecular radius, which is essentially fixed at the scale $a_0 \sim n_0^{-1/3}$, where n_0 is the mean number density. However, by only requiring consistency with the desiderata in Table I—viz. reqs. (2) and (5)—we deduce that a more generally represents a kinetic correlation length, a scale above which a continuum description applies. Indeed, we find the *shape* of $q(k)$, which must depend on the detailed intermolecular potential, strongly influences VACF oscillations, starkly contrasting with the form factor’s largely peripheral role in ensuring normalizability. Note that Eq. (4) implies $q(k) \geq 0$, whereas $\hat{f}(k)$ is negative for a range of wavenumbers; conversely, $q(r) = \int_0^\infty dk k^2 q(k) \sin(kr)/kr$ can oscillate radially about zero, thereby inducing oscillations in the VACF.

The hydrodynamic VACF

For an isotropic fluid, the VACF decomposes into longitudinal and transverse components with respect to wavevector \mathbf{k} as $\psi(t) = \frac{1}{3}\psi_{\parallel}(t) + \frac{2}{3}\psi_{\perp}(t)$; Eq. (3) becomes

$$\psi(t) = \frac{\mathcal{N}_p a^3}{3} \int_0^\infty dk k^2 q(ka) F_s(k, t) [C_{\parallel}(k, t) + 2C_{\perp}(k, t)] \quad (5)$$

where, after changing notation from $q(k)$ to $q(ka)$ and setting $\mathcal{N} = \mathcal{N}_p a^3$, we have explicitly introduced a and a parameter p that controls the shape of $q(ka)$.

Equation (5) and the desiderata in Table I constitute a general formulation of the hydrodynamic VACF. To implement the framework, one specifies the static spectrum, $q(ka)$, and correlation functions, $C_{\parallel, \perp}(k, t)$ and $F_s(k, t)$. In what follows, we develop hydrodynamic models satisfying reqs. (1-6) in Table I to obtain solutions for $C_{\parallel, \perp}(k, t)$ and $F_s(k, t)$. We then introduce representative models for $q(ka)$ that yield simple-fluid VACFs in good agreement with MD calculations.

HYDRODYNAMIC MODEL FORMULATION

To describe *collective* hydrodynamic modes, we develop a *regularized* variant of the well-known 10-moment equations, a relaxation system of partial differential equations (PDEs) that we call *R10*.⁶⁹ When appropriately constrained by the desiderata, R10 reproduces accurate VACFs for simple liquids, as well as realistic VACFs for intermediate-density fluids and gases. Note that R10 is not necessarily the optimal (or unique) hydrodynamic model consistent with the desiderata; in principle, our framework is compatible with other methodologies, including generalized hydrodynamics^{1,72,85} and the GENERIC formalism.^{60,61}

R10 may be obtained from the BGK-Boltzmann equation using the moment method of hydrodynamics, where the BGK relaxation model naturally reproduces the Maxwell model of viscoelasticity in the stress components. We derive analytic expressions for longitudinal and transverse current correlations, which capture damped molecular-scale sound and elastic shear waves, respectively. In particular, the corresponding memory equations and kernels [req. (1)] are *not* assumed, as is commonly done, but rather implied by the R10 PDEs.

To describe the (self-)motion of tagged particle α , we propose a hydrodynamic model for the self-density, n_s , motivated by the R10 equations for collective hydrodynamics variables (n , \mathbf{j} , and \mathbf{S}). We then derive analytic expressions for the SISF via $F_s(k, t) = \langle n_s^*(k, 0) n_s(k, t) \rangle$.

As there are no known exact solutions for F_s , approximations have often leveraged the Gaussian assumption, which is exact in the small- and large- k limits and, conveniently, directly relates to the mean-square displacement (MSD), e.g., $F_s(k, t) = \exp[-\frac{1}{2}k^2 \Delta(t)]$, where $\Delta(t) \equiv \frac{1}{3}\langle|\mathbf{x}_\alpha(t) - \mathbf{x}_\alpha(0)|^2\rangle$ is the MSD of tagged particle α . For instance, a cumulant expansion of $F_s(k, t)$ with a Gaussian leading term directly reveals non-Gaussian effects, which are known to be relatively small for simple liquids.^{1,86} Unlike common approximations, our model for F_s satisfies reqs. (1-6), which, along with our model for C_{\perp} , extends the description to low Schmidt number, $\text{Sc} \equiv \nu/D_s \sim \mathcal{O}(1)$, and reproduces the exponential decay range of gases—a feature not captured by simple diffusion (i.e., Fick’s law) and other Gaussian models.

Regularized 10-moment model (R10)

Consider the following linear transport equations for mass, momentum, and stress for an adiabatic equation of state

$$\partial_t \rho + \nabla \cdot \mathbf{j} = 0 \quad (6)$$

$$\partial_t \mathbf{j} + v_{\parallel}^2 \nabla \rho + \nabla \cdot \mathbf{S} = 0 \quad (7)$$

$$\partial_t \mathbf{S} + 2v_0^2 \dot{\epsilon} = \int d\mathbf{x}' \left[\mathcal{D}(\mathbf{x} - \mathbf{x}') \nabla'^2 - \boldsymbol{\Upsilon}(\mathbf{x} - \mathbf{x}') \right] \cdot \mathbf{S}(\mathbf{x}') \quad (8)$$

where $v_0 = \sqrt{k_B T/m}$ is the thermal speed, v_{\parallel} is the (molecular-scale) longitudinal phase velocity, and $\dot{\epsilon} \equiv \frac{1}{2}[\nabla \mathbf{j} + (\nabla \mathbf{j})^\top - \frac{2}{3}(\nabla \cdot \mathbf{j}) \mathbf{1}]$ is the rate-of-strain tensor. We define the Fourier transform of the collision frequency tensor $\boldsymbol{\Upsilon}(\mathbf{x})$ as

$$\boldsymbol{\Upsilon}_{\mathbf{k}} \equiv \hat{\mathbf{k}} \hat{\mathbf{k}} \gamma + (1 - \hat{\mathbf{k}} \hat{\mathbf{k}}) \nu \quad (9)$$

where $\hat{\mathbf{k}} \equiv \mathbf{k}/k$, $\mathbf{1}$ is the unit tensor, and $\hat{\mathbf{k}} \hat{\mathbf{k}}$ and $1 - \hat{\mathbf{k}} \hat{\mathbf{k}}$ are longitudinal (normal) and transverse (shear) projection operators; γ and ν are the respective collision frequencies. Similarly, for the stress diffusion tensor, $\mathcal{D}(\mathbf{x})$,

$$\mathcal{D}_{\mathbf{k}} \equiv \hat{\mathbf{k}} \hat{\mathbf{k}} \mathcal{D}_{\parallel} + (1 - \hat{\mathbf{k}} \hat{\mathbf{k}}) \mathcal{D}_{\perp} \quad (10)$$

with regularization diffusion coefficients \mathcal{D}_{\parallel} and \mathcal{D}_{\perp} .

Two points should be highlighted. First, the Fourier-transformed collision term, $-\mathbf{\Upsilon}_k \cdot \mathbf{S}_k$, is a relaxation approximation related to the BGK collision operator in the BGK-Boltzmann equation that gives rise to viscoelasticity: e.g., v^{-1} is the transverse component's Maxwell relaxation time. Second, the Fourier-transformed diffusive regularization term, $-k^2 \mathcal{D}_k \cdot \mathbf{S}_k$, extends the description to higher Knudsen (Kn) number^{60,65}—essential for molecular-scale fluid flows where $\text{Kn} \sim \mathcal{O}(1)$ and conventional Navier-Stokes fails.^{87,88} Importantly, *regularization implements moment closure* when constrained by the Green-Kubo relation for self-diffusion [req. (7)], as well as eliminating spatial structure below physically meaningful scales [req. (4)].

Relaxation limit of the stress components

Working in Fourier space, the transverse projection of Eqs. (7) and (8) yields

$$\frac{d\mathbf{j}_{\perp k}}{dt} = -ik \cdot \mathbf{S}_{\perp k} \quad (11)$$

$$\frac{d\mathbf{S}_{\perp k}}{dt} + (v + k^2 \mathcal{D}_{\perp}) \mathbf{S}_{\perp k} = -iv_0^2 \mathbf{k} \mathbf{j}_{\perp k} \quad (12)$$

while the longitudinal projection of Eqs. (6) to (8) yields

$$\frac{d\rho_k}{dt} = -ik \cdot \mathbf{j}_{\parallel k} \quad (13)$$

$$\frac{d\mathbf{j}_{\parallel k}}{dt} = -iv_{\parallel}^2 \mathbf{k} \rho_k - ik \cdot \mathbf{S}_{\parallel k} \quad (14)$$

$$\frac{d\mathbf{S}_{\parallel k}}{dt} + (\gamma + k^2 \mathcal{D}_{\parallel}) \mathbf{S}_{\parallel k} = -iv_0^2 \left(\frac{1}{3} \mathbf{k} \mathbf{j}_{\parallel k} + \mathbf{j}_{\parallel k} \mathbf{k} \right) \quad (15)$$

We then make the key assumption that the longitudinal stress relaxation rate, $\gamma + k^2 \mathcal{D}_{\parallel}$, is faster than any other timescale, which circumvents solving a third-order differential equation for C_{\parallel} and proves to be a good approximation; Eq. (15) relaxes to

$$\mathbf{k} \cdot \mathbf{S}_{\parallel k} = -i\mu_k \mathbf{k} \mathbf{k} \cdot \mathbf{j}_{\parallel k} \quad (16)$$

where $\mu_k \equiv \frac{4}{3}v_0^2/(\gamma + k^2 \mathcal{D}_{\parallel})$ is a k -dependent kinematic bulk viscosity. Here, γ is determined in the small- k limit from available data for the bulk viscosity, $\mu \equiv v_0^2/\gamma$, and \mathcal{D}_{\parallel} is treated as a free parameter; the intuitive choice $\mathcal{D}_{\parallel} \rightarrow 4\mu/3$ yields good results for present calculations.

It is instructive to note that the *isotropic* relaxation limit (i.e., $\gamma = v$, $v \gg \partial_t$, and $v \gg k^2 \mathcal{D}_{\perp}$) yields the linearized Navier-Stokes equations with *steady-state* kinematic viscosity $\nu = v_0^2/v$, where the stress equation relaxes to Newton's law of viscosity, $\mathbf{S} = -2\nu \dot{\mathbf{\epsilon}}$.

Modal current correlation functions

Using Eqs. (11) and (12) for the transverse component, and the relaxation approximation for the longitudinal

component, Eqs. (13), (14) and (16), we derive ordinary differential equations (ODEs) in time for the modal correlation functions using $\mathbf{j}_k(t) = \rho_0 \mathbf{u}_k(t)$. For transverse current correlations, C_{\perp} , we combine Eqs. (11) and (12) to obtain a second-order ODE for the transverse current

$$\frac{d^2 \mathbf{j}_{\perp k}}{dt^2} + (v + k^2 \mathcal{D}_{\perp}) \frac{d\mathbf{j}_{\perp k}}{dt} + k^2 v_0^2 \mathbf{j}_{\perp k} = 0 \quad (17)$$

which leads to

$$\ddot{C}_{\perp}(k, t) + v_k \dot{C}_{\perp}(k, t) + k^2 v_0^2 C_{\perp}(k, t) = 0 \quad (18)$$

where $v_k \equiv v + k^2 \mathcal{D}_{\perp}$. Equation (18) has a memory equation form, req. (1), with kernel $K_{\perp}(k, t) = k^2 v_0^2 \exp(-v_k t)$. Similarly, substitution of the relaxation limit, Eq. (16), into Eq. (14) eventually yields a second-order ODE for the longitudinal current correlations

$$\ddot{C}_{\parallel}(k, t) + \gamma_k \dot{C}_{\parallel}(k, t) + k^2 v_0^2 C_{\parallel}(k, t) = 0 \quad (19)$$

where $\gamma_k \equiv k^2 \mu_k$. With the initial conditions $C_{\parallel, \perp}(k, 0) = 1$ and $\dot{C}_{\parallel, \perp}(k, 0) = 0$ [reqs. (2–3)], solutions to Eqs. (18) and (19) are readily found:

$$C_{\perp}(k, t) = \frac{1}{2} e^{-\frac{1}{2}v_k t} \left[\left(1 - \frac{v_k}{\alpha_k} \right) e^{-\frac{1}{2}\alpha_k t} + \left(1 + \frac{v_k}{\alpha_k} \right) e^{\frac{1}{2}\alpha_k t} \right] \quad (20)$$

$$C_{\parallel}(k, t) = \frac{1}{2} e^{-\frac{1}{2}\gamma_k t} \left[\left(1 - \frac{\gamma_k}{\beta_k} \right) e^{-\frac{1}{2}\beta_k t} + \left(1 + \frac{\gamma_k}{\beta_k} \right) e^{\frac{1}{2}\beta_k t} \right] \quad (21)$$

where $\alpha_k \equiv \sqrt{v_k^2 - 4k^2 v_0^2}$ and $\beta_k \equiv \sqrt{\gamma_k^2 - 4k^2 v_{\parallel}^2}$. Equations (20) and (21) have the flexibility to satisfy all requirements in Table I; the corresponding dynamic spectral densities are provided in Appendix A.

Self-intermediate scattering function

The regularized relaxation models represented by Eqs. (11) and (12) and Eqs. (13) to (15) for the collective hydrodynamic variables suggest the following model

$$\frac{dn_s}{dt} = -ik \cdot \mathbf{j}_s \quad (22)$$

$$\frac{d\mathbf{j}_s}{dt} + (\gamma_s + k^2 D_s) \mathbf{j}_s = -ik v_0^2 n_s \quad (23)$$

where $n_s(k, t)$ is the (self-)density of a *non-interacting* collection of tagged particles (i.e., test particles⁸⁶), $\mathbf{j}_s(k, t)$ the self-current, γ_s the Brownian collision frequency corresponding to (Stokes) friction, and D_s the self-diffusion coefficient; here, we take $D_s \rightarrow v_0^2/\gamma_s$, which enforces req. (4) and ensures the positivity of F_s for all k and t .

Equations (22) and (23) are a natural generalization of Fick's Law of self-diffusion,^{54,55} which is recovered in the full relaxation limit ($\gamma_s \rightarrow \infty$, $k \rightarrow 0$) where Eqs. (22)

and (23) reduce to a diffusion equation for $n_s(k, t)$. The full ODE corresponding to Eqs. (22) and (23) is

$$\ddot{F}_s(k, t) + (\gamma_s + k^2 D_s) \dot{F}_s(k, t) + k^2 v_0^2 F_s(k, t) = 0 \quad (24)$$

the roots of which factor nicely to give

$$F_s(k, t) = \frac{\gamma_s e^{-k^2 D_s t} - k^2 D_s e^{-\gamma_s t}}{\gamma_s - k^2 D_s} \quad (25)$$

Note that density fluctuations decay exponentially for large k . To see that this model is reasonable, consider Eq. (24) in memory equation form

$$\dot{F}_s(k, t) + k^2 v_0^2 \int_0^t dt' e^{-\gamma_{sk}(t-t')} F_s(k, t') = 0 \quad (26)$$

where $\gamma_{sk} = \gamma_s + k^2 D_s$, $\gamma_s > 0$. The Markovian solution, obtained by freezing $F_s(k, t')$ at the upper limit t , is

$$F_s(k, t) = \exp \left[-k^2 \left(\frac{v_0}{\gamma_{sk}} \right)^2 \left(\gamma_{sk} t + e^{-\gamma_{sk} t} - 1 \right) \right] \quad (27)$$

which, when $D_s = 0$, yields the formal result for conventional Langevin dynamics.¹ Also note that when $D_s \rightarrow 0$ in Eq. (25), $F_s(k, t) \rightarrow 1$ and Eq. (27) would not satisfy req. (4). It is unsurprising that $D_s > 0$ is necessary for a physically meaningful SISF.

IMPLEMENTATION OF THE FRAMEWORK

The VACF is calculated by evaluating Eq. (5) using the normalized transverse and longitudinal current correlations, Eq. (20) and Eq. (21), and SISF, Eq. (25), along with the static spectrum, $q(ka)$, discussed subsequently; importantly, all VACF calculations utilize these equations (and parameters). However, parameter determination for gases (Appendix D) is considerably more complicated since the short-time sum rule [req. (5)] only applies to dense fluids, $F_s \approx 1$ cannot be assumed for req. (7), and empirical data for transport parameters is limited. A suitable kinetic theory, such as Enskog theory (used here) or modifications thereof,^{89–91} can be used with our framework to derive sum rules connecting molecular parameters to macroscopic quantities,^{10,92} as well as estimating transport coefficients in lieu of empirical inputs.

Static spectrum

Pending a first-principles derivation of $q(ka)$, we consider representative two-parameter models: a symmetric generalized Gaussian

$$q_G(ka) = \mathcal{N}^G v_0^2 e^{-\frac{1}{2}|ka|^p} \quad (28)$$

with $p \geq 1$, and generalized Lorentzian

$$q_L(ka) = \mathcal{N}^L \frac{v_0^2}{1 + |ka|^p} \quad (29)$$

Table II. Key parameters. Left two columns: relations and constraints for molecular parameters. Right three columns: input data for liquid rubidium/argon calculations in Figs. 1 and 2.

Param.	Expr.	Input	Value	
ν	η/ρ_0	T	319.0 K ⁹⁵	87.0 K ⁵⁷
μ	η_b/ρ_0	ρ_0	1500.0 kg/m ³ ⁹⁵	1430.0 kg/m ³ ⁵⁷
v_0	v_0^2/ν	η	644.0 μ Pa·s ⁹⁶	290.0 μ Pa·s ⁹⁷
γ_0	v_0^2/μ	η_b	2020 μ Pa·s ⁹⁸	90.0 μ Pa·s ⁹⁹
γ_{s0}	v_0^2/D_s	D_s	$2.85 \cdot 10^{-9}$ m ² /s ¹⁰⁰	$1.75 \cdot 10^{-9}$ m ² /s ¹⁰¹
a	req. (5)	ω_E	6.1 ps ⁻¹ ⁵⁶	7.7 ps ⁻¹ ²⁴
v, γ, γ_s	req. (6)	v_\parallel^2	1.8 v_0^2 ^a	2.4 v_0^2 ^a
\mathcal{D}_\perp	req. (7)	p	14 ^a	2 ^a
\mathcal{D}_\parallel		$4\mu/3$ $q(ka)$	$q_L(ka)$ ^b	$q_G(ka)$ ^b

^aFree model parameter

^bSee Eqs. (28) and (29).

with $p \geq 6$, where the normalizations depend on shape parameter p via $\mathcal{N}^G \equiv \mathcal{N}_p^G a^3$ and $\mathcal{N}^L \equiv \mathcal{N}_p^L a^3$. Equations (28) and (29) approach the equipartition spectrum for small a ; softer intermolecular potentials correspond to sharper spectral cutoffs (larger p), which amplify oscillations in the VACF [cf. Fig. 1].^{93,94} Note that normalization [req. (2)] yields $\mathcal{N}_p^G = p/[8^{1/p} \Gamma(3/p)]$, whereas solutions for \mathcal{N}_p^L are unavailable for general p , so Eq. (28) is preferred for analytic manipulation.

Parameter determination for liquids

The short- [req. (5)] and long-time [req. (6)] behavior of the VACF uniquely determines a and relaxation frequencies v and γ_s . To see this, consider the long-time behavior by evaluating Eq. (5) with the asymptotic forms $C_\perp(k, t) \sim \exp[-k^2(v_0^2/v)t]$ and $F_s(k, t) \sim \exp[-k^2(v_0^2/\gamma_s)t]$

$$\psi(t) \sim \frac{2}{3} \mathcal{N}_p a^3 \int_0^\infty dk k^2 q(ka) e^{-k^2(v_0^2/\gamma_s)t} e^{-k^2(v_0^2/v)t} \quad (30)$$

$$\sim \frac{\sqrt{\pi} \mathcal{N}_p}{6} \left[\frac{v_0^2}{a^2} \left(\frac{1}{v} + \frac{1}{\gamma_s} \right) t \right]^{-3/2} \quad (31)$$

along with the theoretical prediction from mode-coupling^{54,55,102} and kinetic theory^{103,104}

$$\psi(t) \sim \frac{2}{3n_0} \left[\frac{1}{4\pi(\nu + D_s)t} \right]^{3/2} \quad (32)$$

Naively, one can match Eq. (32) by assuming $v \rightarrow v_0^2/\nu$, $\gamma_s \rightarrow v_0^2/D_s$, and $\sqrt{\pi} \mathcal{N}_p a^3/6 \rightarrow (2/3n_0)(4\pi)^{-3/2}$. This satisfies req. (6) and implies $a \rightarrow a_0 \equiv (2\pi^2 \mathcal{N}_p n_0)^{-1/3}$. But the short-time sum rule [req. (5)] generally yields $a \leq a_0$ (cf. Appendix B), implying that the molecular-scale parameters $v \neq v_0^2/\nu$ and $\gamma_s \neq v_0^2/D_s$. Assigning

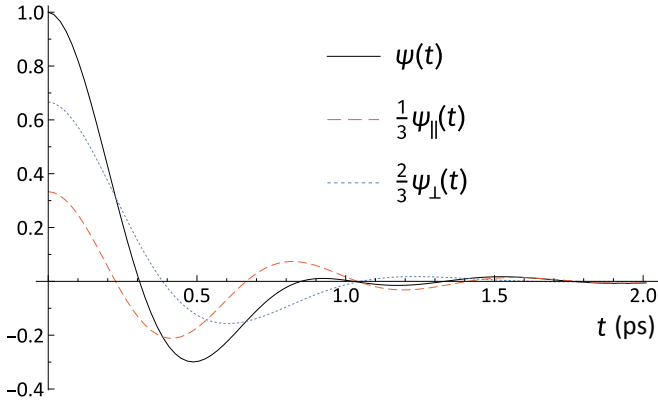


FIG. 1. Liquid rubidium VACF ($T \approx 319$ K, $\rho_0 \approx 1.51 \cdot 10^3$ kg/m 3) with longitudinal (orange) and transverse (blue) components, using a generalized Lorentzian static spectrum ($p = 14$).

consistent values for a , v , and γ_s therefore requires a more careful procedure to concomitantly satisfy reqs. (5) and (6). Importantly, treating the products a^2v and $a^2\gamma_s$ in Eq. (31) as invariant quantities preserves the asymptotic form.

These observations suggest the following procedure. First, define the following “base” values: $v_0 \equiv v_0^2/\nu$ and $\gamma_{s0} \equiv v_0^2/D_s$ (cf. Table II). Second, determine a through the short-time sum rule. E.g., for a generalized Gaussian spectrum, one obtains (cf. Appendix B)

$$a^2 = \frac{4^{1/p}\Gamma(5/p)}{\Gamma(3/p)} \times \frac{1}{3\omega_E^2} (v_{\parallel}^2 + 2v_0^2) \quad (33)$$

Finally, take $v \rightarrow (a_0/a)^2 v_0$ and $\gamma_s \rightarrow (a_0/a)^2 \gamma_{s0}$, which preserves Eq. (32). Consistency suggests the longitudinal collision frequency be rescaled accordingly: $\gamma \rightarrow (a_0/a)^2 \gamma_0$, where $\gamma_0 \equiv v_0^2/\mu$.

Parameter determination at lower densities

Given the paucity of numerical and experimental data for dilute monatomic fluids, we determine inputs using Enskog theory supplemented by heat capacity data from the National Institute of Standards and Technology (NIST) Chemistry WebBook.⁹⁷ For brevity, procedural details are provided in Appendix D.

NUMERICAL RESULTS

VACF calculations for liquid rubidium and argon use values listed in Table II. Calculations for lower densities are consistent with gaseous and supercritical argon where, as proof of principle, we use expressions for the Enskog viscosity and diffusion coefficients combined with reqs. (4) and (7) to derive reasonable values for the key parameters D_{\perp} , v , γ_s , and a (cf. Appendix D).

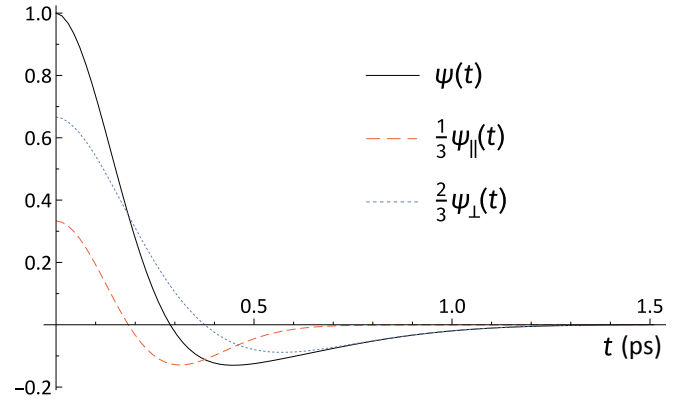


FIG. 2. Liquid argon VACF near the triple point ($T \approx 87$ K, $\rho_0 \approx 1.43 \cdot 10^3$ kg/m 3) with longitudinal (orange) and transverse (blue) components, using a Gaussian static spectrum ($p = 2$).

Figure 1 shows the VACF for liquid rubidium using a generalized Lorentzian spectrum with $p = 14$, which should be compared to the velocity-field results (Ref. 56, Fig. 1; Ref. 81, Fig. 2). The oscillatory VACF behavior of liquid alkali metals observed in MD simulations^{56,57,81,105} requires a relatively sharp cutoff (large p), which corresponds to the relatively soft repulsive core of the intermolecular potential as compared to Lennard-Jones-like fluids.^{78,93,94}

Figure 2 shows the VACF for liquid argon near the triple point using a Gaussian ($p = 2$) spectrum (cf. velocity-field results: Ref. 57, Fig. 2). We remark that the plateau often seen in MD calculations of the liquid argon VACF can be reasonably reproduced in our formulation by using a generalized Lorentzian spectrum with $p \approx 7.5$, $v_{\parallel}^2 \approx 3.0v_0^2$, and adjusting D_s upward by $\sim 10\%$ so as to increase oscillations primarily in the *longitudinal* (but not transverse) component.

Figure 3 shows representative VACF calculations for hard-sphere gaseous and supercritical fluids based on argon parameters. The exponential and diffusive ($t^{-3/2}$) decay ranges are a direct consequence of the explicit handoff in Eq. (25) and Eq. (D3). These prominent features were clearly observed in hard-sphere MD simulations by Zhao and Zhao³² and are also evident in MD calculations for a supercritical Lennard-Jones (LJ) fluid,²⁸ immersed-particle fluctuating hydrodynamics simulations at low Sc ,^{53,106,107} and analytic calculations for Basset-Boussinesq-Oseen (BBO) dynamics^{12,108–111} with general slip boundary conditions.¹¹² In particular, the dips seen in Fig. 3 at early times comes from the longitudinal current, which appears to capture the effect of strongly damped sound waves. Similar features are clearly evident in MD calculations: see Ref. 32, Fig. S1 and also Appendix E for an indirect comparison with Ref. 28, Fig. 1, which shows excellent quantitative agreement. Analytic calculations for “BBO particles”¹¹³ also exhibit qualitative similarities (Ref. 112, Figs. 2 and 3).

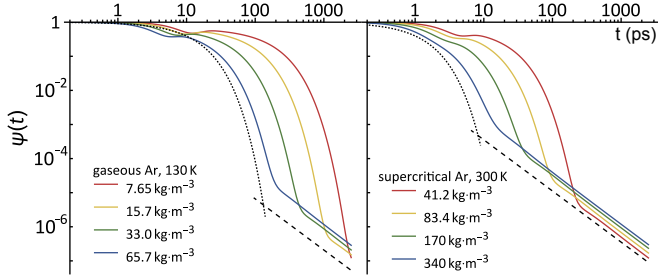


FIG. 3. Hard-sphere VACFs emulating gaseous (left) and supercritical (right) argon ranging from low (red) to high (blue) densities. Pure exponential (dotted) and $t^{-3/2}$ (dashed) decay are shown as guides to the eye. Note that at 300 K, 41.2 kg/m³ (right, red) argon is *gaseous* (and not supercritical).

DISCUSSION

The present theory reflects an eclectic synthesis of ideas dispersed throughout the literature along with several new concepts. We have organized the theoretical formulation and framework in this Communication so as to highlight important results. In summary, we:

- (1) Presented a new derivation and interpretation of the hydrodynamic VACF formulation, Eqs. (2) to (5).
- (2) Established a core set of physical desiderata whose constraints are sufficient to recover realistic VACFs.
- (3) Identified $q(ka)$ as the initial condition of the (un-normalized) current correlation function, which characterizes molecular-scale kinetic fluctuations and reproduces the VACF over *all* timescales by judiciously superimposing each hydrodynamic mode.
- (4) Proposed linear hydrodynamic PDEs (R10) to model collective modes, yielding analytic solutions for $C_{\perp}(k, t)$ and $C_{\parallel}(k, t)$ having sufficiently rich and complex structure to resolve subtle details of the VACF.
- (5) Proposed a new hydrodynamic model for the self-density, leading to a new, general form for the self-intermediate scattering function, $F_s(k, t)$.
- (6) Described the (re-)scaling of hydrodynamic model parameters that recover the short-time VACF behavior while preserving the long-time asymptotics.

We have argued that regularization, which induces hydrodynamic closure via the Green-Kubo relation [req. (7)], is essential, particularly so at low densities. Importantly, Eq. (25) shows that exponential decay occurs when $k^2 D_s > \gamma_s$, which implies $k\lambda_E > 1$ where $\lambda_E \sim v_0/\gamma_s$ is the Enskog mean-free path. More precisely, when $a < k^{-1} < \lambda_E$, the expected exponential decay range of a gas emerges from the contributions of large- k modes. Also note that the slowest relaxation rate of $C_{\perp}(k, t)$ is given by the smaller of the two exponents in Eq. (20), which, when expanded for large k , gives $-v_0^2/\mathcal{D}_{\perp}$ when $\mathcal{D}_{\perp} > 0$. This shows the regularization coefficients \mathcal{D}_{\perp} and D_s are essential at low densities.

The Einstein frequency, ω_E , becomes ill-defined as density is lowered, which appears to coincide with the emergence of exponential ranges in F_s and C_{\perp} , suggesting a natural dynamical criterion delineating the transition to the vapor phase. In particular, the corresponding non-Gaussian behavior of the VACF at intermediate times, which switches from damped oscillations to pure exponential decay, may lend dynamical insight into the liquid-gas phase transition not otherwise available through other methods. Realizing such a fully capable VACF theory would require a means to determine a as a continuous function of density (and temperature) through the phase transition without relying solely on ω_E and the short-time sum rule [req. (5)]. Our methodology is nevertheless flexible since molecular parameters can be determined via alternative kinetic models, as illustrated by our gaseous and supercritical argon calculations using Enskog theory.

It is worth mentioning that one can derive telegrapher's equations from R10 for $\mathcal{D}_{\perp} = 0$. In fact, Trachenko¹¹⁴ derived a telegrapher's equation as a liquid dynamics model by generalizing solid-like equations. We remark that telegrapher's equations describe *persistent* random walks, which accounts for directional correlations in Brownian motion.^{115–117} Indeed, as pointed out by Khrapak,¹¹⁸ Zwanzig's speculative model of molecular self-motion in a liquid¹¹⁹—where collective rearrangements correspond to configurational transitions between metastable equilibria—is consistent with the persistent random walk picture. From a hydrodynamic standpoint, this persistence originates from the finite relaxation time of molecular-scale fluid stresses.

We expect the present theory to be useful well beyond the VACF calculations themselves. For example, Alder and Wainwright⁶ and, more recently, Han *et al.*³⁰ and Lesnicki and Vuilleumier,¹²⁰ have convincingly demonstrated that collective motions in discrete-particle systems are well represented by hydrodynamic flow fields down to the molecular scale. This suggests that stochastically driven R10 equations,⁸⁸ which generalize the Landau-Lifschitz Navier-Stokes equations,¹²¹ may represent a viable molecular-hydrodynamic model capable of reproducing molecular-scale streamline plots. Indeed, the efficacy of our hydrodynamic VACF formulation is largely enabled by $q(ka)$, which must ultimately originate from kinetic fluctuations.

Other avenues to explore include analyzing the full third-order ODE system for $C_{\parallel}(k, t)$ (i.e., away from the relaxation limit), implementing a full numerical solution to the zero-frequency constraint for \mathcal{D}_{\perp} [i.e., req. (7) with $F_s \neq 1$], and deriving $q(ka)$ from first principles. In addition, the emergence of an exponential range at lower densities, which is enabled by our novel hydrodynamic model for n_s , highlights the connection to general Brownian motion involving a (larger) particle immersed in a bath of (smaller) solvent particles.¹²² In particular, Zhao and Zhao³² also used MD to calculate VACFs for large Brownian particles, encouraging deeper examination of

the putative connection to tagged-particle equations of motion, such as the fluctuating BBO equation^{123–125} and other generalized Langevin equations (GLEs). Memory kernel reconstruction methods^{36,38,41} for GLEs may, for instance, enable data-driven insights into these connections, as well as helping extend the present methodology to driven hydrodynamic Brownian motion in complex fluids.^{113,125–132} Also fruitful would be to explore applications to supercooled,^{133–136} supercritical,^{137–139} and ionic and dielectric fluids.^{76,140–145}

ACKNOWLEDGMENTS

The authors are grateful for valuable discussions with Mark A. Hayes, Dmitry Matyushov, Jason Hamilton, Ralph V. Chamberlin, Paul Campitelli, and Kyle L. Seyler. SLS would like to warmly acknowledge Oliver Beckstein and the Blue Waters Graduate Fellowship program—a part of the Blue Waters sustained-petascale computing project supported by the National Science Foundation (awards OCI-0725070 and ACI-1238993) and the state of Illinois—whose generous support helped nucleate this research; Blue Waters is a joint effort of the University of Illinois at Urbana-Champaign and its National Center for Supercomputing Applications. CES was supported by the National Nuclear Security Administration Stewardship Sciences Academic Programs under Department of Energy Cooperative Agreement No. DE-NA0003764.

AUTHOR DECLARATIONS

Conflict of Interest

The authors have no conflicts to disclose.

Author Contributions

All authors contributed equally to this work.

DATA AVAILABILITY

The data that support the findings of this study are available within the article and its supplementary material.

Appendix A: Dynamic spectral densities

The dynamic structure factor $J(k, \omega)$ is the cosine transform of the current correlation function.

$$J(k, \omega) = 2 \int_0^\infty dt C(k, t) \cos(\omega t) \quad (A1)$$

Recalling that $v_k \equiv v + k^2 \mathcal{D}_\perp$ and $\gamma_k \equiv \gamma + k^2 D_\parallel$, we find for the transverse and longitudinal correlations respectively

$$J_\perp(k, \omega) = \frac{2k^2 v_0^2 v_k}{(\omega^2 - k^2 v_0^2)^2 + \omega^2 v_k^2} \quad (A2)$$

$$J_\parallel(k, \omega) = \frac{2k^2 v_\parallel^2 \gamma_k}{(\omega^2 - k^2 v_\parallel^2)^2 + \omega^2 k^4 \mathcal{D}_\parallel^2} \quad (A3)$$

Note the following property: as $v_k, \gamma_k \rightarrow 0$ and $\mathcal{D}_\perp, D_\parallel \rightarrow 0$, the spectral densities approach delta functions in the arguments $\omega = \pm k v_0$ and $\omega = \pm k v_\parallel$. Compare these results to purely viscous decay that one would obtain from the Navier-Stokes equation

$$J_{NS}(k, \omega) = \frac{2k^2 \nu}{\omega^2 + k^4 \nu^2} \quad (A4)$$

Appendix B: Determination of scale a for liquids [req. (5)]

In sufficiently dense fluids such as a liquid, the Einstein frequency, ω_E , has physical relevance and a can be computed from the second-moment condition by considering the short-time expansion of the VACF

$$\psi(t) = 1 - \frac{1}{2} \left(\frac{t}{\tau_c} \right)^2 + \dots = 1 - \frac{1}{2} \omega_E^2 t^2 + \dots \quad (B1)$$

where $\tau_c = \omega_E^{-1}$ is the timescale characterizing the initial (de)correlation of the VACF and the Einstein frequency, ω_E , is formally defined via

$$\omega_E^2 \equiv \frac{4\pi n_0}{3m} \int_0^\infty dr r^2 g(r) \left(\frac{d^2 \phi}{dr^2} + \frac{2}{r} \frac{d\phi}{dr} \right) \quad (B2)$$

where $g(r)$ is the radial distribution function and $\phi(r)$ is the intermolecular potential. For large Sc—assumed to be the case for liquids—the short-time expansion of the modal correlation function dominates that from the self-intermediate scattering function. That is, when $\nu \gg D_s$, we have $v_0^2/v \gg v_0^2/\gamma_s$ and then $\gamma_s \gg v$. Thus, in the liquid state, $F_s(k, t) \approx 1$ over the timescale τ_c and the initial decay of the VACF (and the location of the first zero-crossing) is controlled by the modal current correlation functions, C_\perp and C_\parallel .

The integrand of the hydrodynamic VACF formula, Eq. (5), can thus be approximated as

$$F_s(k, t) C(k, t) \approx 1 - \frac{1}{2} k^2 \left(\frac{1}{3} v_\parallel^2 + \frac{2}{3} v_0^2 \right) t^2 \quad (B3)$$

and so the short-time VACF is approximately

$$\psi(t) \approx \frac{N_p a^3}{3} \int_0^\infty dk k^2 q(ka) \left[1 - \frac{1}{2} k^2 \left(v_\parallel^2 + 2v_0^2 \right) t^2 \right] \quad (B4)$$

Equating the quadratic terms in Eq. (B1) and Eq. (B4), we obtain

$$\omega_E^2 = \frac{\mathcal{N}_p a^3}{3} \int_0^\infty dk k^4 q(ka) (v_\parallel^2 + 2v_0^2) \quad (\text{B5})$$

which is the second frequency-moment condition (i.e., f -sum rule).³

To obtain Eq. (33), explicitly evaluate Eq. (B5) for the generalized Gaussian spectrum

$$\psi(t) = \frac{pa^3}{8^{1/p}\Gamma(3/p)} \int_0^\infty dk k^2 e^{-\frac{1}{2}|ka|^p} F_s(k, t) C(k, t)$$

The scale a can now be deduced from the correlation time τ_c through the second wavenumber moment of the static spectrum, $q(k)$:

$$\omega_E^2 = \frac{pa^3 v_a^2}{8^{1/p}\Gamma(3/p)} \int_0^\infty dk k^4 e^{-\frac{1}{2}|ka|^p} \quad (\text{B6})$$

where $v_a^2 \equiv (v_\parallel^2 + 2v_0^2)/3$. Carrying out the integral analytically and rearranging to solve for a yields

$$a = \sqrt{\frac{4^{1/p}\Gamma(5/p)}{\Gamma(3/p)}} \frac{v_a}{\omega_E} \quad (\text{B7})$$

which agrees with Eq. (33). For the specific case of a pure Gaussian static spectrum, $a = \sqrt{3}v_a/\omega_E$. In the liquid state, it is seen that the main decay timescale is controlled by the molecular scale a via $\tau_c = \omega_E^{-1} \sim a/v_a$.

Appendix C: Zero-frequency constraint for liquids [req. (7)]

The Green-Kubo relation for self-diffusion is

$$D_s = v_0^2 \int_0^\infty dt \psi(t) \quad (\text{C1})$$

In the liquid regime, it is reasonable to take $C_\parallel(k, t) \rightarrow 0$ and $F_s(k, t) \rightarrow 1$, which allows us to evaluate Eq. (C1) analytically using Eq. (5) to obtain

$$D_s = \frac{2}{3} [\mathcal{D}_\perp + \chi(p)a^2 v] \quad (\text{C2})$$

where $\chi(p)$ is a coefficient that depends on the sharpness of the spectral cutoff. After rearranging, we obtain

$$\mathcal{D}_\perp = \frac{3}{2} D_s - \chi(p)a^2 v \quad (\text{C3})$$

which, as shown below, yields analytic constraints for \mathcal{D}_\perp when D_s is known (e.g., experimentally) and the static spectrum is represented by either the generalized Gaussian or Lorentzian forms [Eqs. (28) and (29)].

For the transverse current, Eq. (C1) becomes

$$D_s = \frac{2}{3} v_0^2 \mathcal{N} \int_0^\infty dk k^2 q(ka) \int_0^\infty dt C_\perp(k, t) \quad (\text{C4})$$

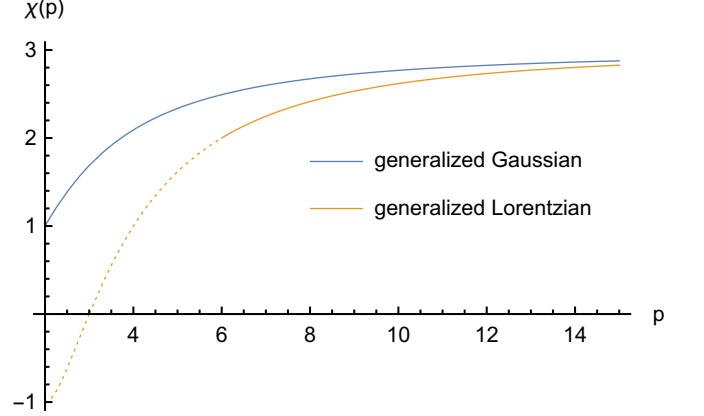


FIG. C.1. Coefficient $\chi(p)$ in Eq. (C9) from the transverse component's contribution to the long-time diffusivity for generalized Gaussian, Eq. (28), and Lorentzian, Eq. (29), static spectrum functions. The dashed line indicates values of p for which the second-moment k -integral [req. (5a)] is divergent for the generalized Lorentzian spectrum (i.e., $p < 6$).

Carrying out the time integration first yields

$$v_0^2 \int_0^\infty dt C_\perp(k, t) = \mathcal{D}_\perp + \frac{v}{k^2} \quad (\text{C5})$$

so that the k -integral that remains to be evaluated is

$$I_\perp [q(ka)] = \frac{2}{3} \mathcal{N}_p a^3 \int_0^\infty dk k^2 q(ka) \left(\mathcal{D}_\perp + \frac{v}{k^2} \right) \quad (\text{C6})$$

For a generalized Gaussian spectrum, Eq. (C6) becomes

$$\frac{3}{2} I_\perp \left[e^{-\frac{1}{2}(ka)^p} \right] = \mathcal{D}_\perp + \frac{1}{4^{1/p} \Gamma(3/p)} a^2 v \quad (\text{C7})$$

and, for a generalized Lorentzian,

$$\frac{3}{2} I_\perp \left[\frac{1}{1 + (ka)^p} \right] = \mathcal{D}_\perp + \frac{\csc(\pi/p)}{\csc(3\pi/p)} a^2 v \quad (\text{C8})$$

Inspection of Eqs. (C7) and (C8) reveals that the transverse current correlation uniquely contributes a p -dependent coefficient of the $a^2 v$ term, $\chi(p)$, unlike the longitudinal current correlation, as well as depending on the functional form of $q(ka) = q_p(ka)$:

$$\frac{3}{2} D_s = \frac{3}{2} I_\perp [q_p(ka)] = \mathcal{D}_\perp + \chi(p)a^2 v \quad (\text{C9})$$

Thus, \mathcal{D}_\perp can be readily computed using Eq. (C7) or Eq. (C8) with Eq. (C3).

Figure C.1 compares the magnitude of $\chi(p)$ for the generalized Gaussian (blue) and generalized Lorentzian (orange) forms for the static spectrum. It is seen, for instance, that a generalized Gaussian with $p = 4$ gives roughly the same contribution to the overall diffusivity as the generalized Lorentzian with $p \approx 6$.

Appendix D: Parameter determination for dilute fluids

Regularization and the exponential range [req. (4)]. At lower densities, self-diffusion becomes important and Sc is relatively small as compared to the liquid case. For a dilute gas, where $\text{Sc} \sim \mathcal{O}(1)$, it would be reasonable to assume the exponential range [req. (4)] arises only from the product $F_s(k, t)C_\perp(k, t)$. Then, one might define an *effective* decay rate, Ω_0 , to be the sum of the SISF and transverse current collision rates, i.e., $\Omega_0 = \gamma_s + v$. It will be shown below that this assumption is not unreasonable and can be formally justified by enforcing req. (7) using large- k approximations for the correlation functions. Specifically, the exponential range should arise for values of k where $kv_0 > \tau$ and $\Omega_0 = \tau^{-1}$ [req. (4)]. Indeed, unlike in the liquid case, the SISF cannot be treated as approximately constant (i.e., $F_s \neq 1$) over the time interval with the dominant contribution to self-diffusion, which precludes an exact analytic integration over k . However, for dilute monatomic gases, the dominant contribution to D_s generally comes from the large- k forms of $C_\perp(k, t)$ and $F_s(k, t)$, in the Green-Kubo relation allowing an approximate k integration.

In this scenario, regularization plays a critical role, as seen by considering the slowest relaxation rate of $C_\perp(k, t)$ —the smaller of the two exponents in Eq. (20), which, for large k , is

$$-\frac{1}{2}v_k + \frac{1}{2}\sqrt{v_k^2 - 4k^2v_0^2} \sim -\frac{k^2v_0^2}{v + k^2\mathcal{D}_\perp} \sim -\frac{v_0^2}{\mathcal{D}_\perp} \quad (\text{D1})$$

This relaxation rate must be finite as $k \rightarrow \infty$ [req. (4)], which, evidently, necessitates the inclusion of the regularization diffusion coefficient, \mathcal{D}_\perp . A similar argument holds for the exponential range of $F_s(k, t)$, where D_s is the corresponding regularization coefficient.

Similarly, the longitudinal relaxation rate for large- k is $\sim v_{\parallel}^2/\mu$; however, the bulk viscosity of a dilute monatomic gas is typically very small compared to its shear viscosity,^{146–148} making its contribution to the diffusivity small as well. To see this analytically, consider the VACF with a Gaussian static spectrum ($p = 2$) and bulk viscosity set to zero: the longitudinal contribution is the rapidly decaying form $\psi_{\parallel}(t) \sim (1 - v_{\parallel}^2 t^2/a^2) \exp(-v_{\parallel}^2 t^2/2a^2)$, which integrates exactly to zero. Thus, while C_{\parallel} can affect the short-time VACF structure, only C_\perp and F_s dictate the exponential range and overall diffusivity under dilute conditions.

Zero-frequency constraint [req. (7)]. Excluding the longitudinal component, the Green-Kubo relation for large k becomes [req. (7)]

$$D_s = \frac{2}{3}v_0^2 \left(\gamma_s + \frac{v_0^2}{\mathcal{D}_\perp} \right)^{-1} \quad (\text{D2})$$

Note the appearance of the additional parameter γ_s due to the treatment of finite Sc . To obtain uniquely determined parameters, we now require a separate relation between \mathcal{D}_\perp and v or another way to determine γ_s . At present, it seems reasonable to assume

$\mathcal{D}_\perp \rightarrow v_0^2/v$, which is consistent with the assumption that $D_s \rightarrow v_0^2/\gamma_s$, which was used in Eqs. (22) to (25)—the equations for the self-density and SISF. We remark that when $\mathcal{D}_\perp = v_0^2/v$, the roots of Eq. (18) factor nicely to give

$$C_\perp(k, t) = \frac{ve^{-k^2\mathcal{D}_\perp t} - k^2\mathcal{D}_\perp e^{-vt}}{v - k^2\mathcal{D}_\perp} \quad (\text{D3})$$

matching the neat form of Eq. (25) and preserving the positivity of the VACF in accordance with what is expected for a dilute gas.

Setting $\mathcal{D}_\perp = v_0^2/v$ in Eq. (D2), we now have

$$D_s = \frac{2}{3} \frac{v_0^2}{\gamma_s + v} \quad (\text{D4})$$

Clearly, we cannot directly set $D_s = v_0^2/\gamma_s$ on the left-hand side of Eq. (D4), as there would be no positive solution for v . We instead conjecture that γ_s represents the *rescaled* (self-)collision frequency, while γ_{s0} is its corresponding *base* value determined by $D_s \equiv v_0^2/\gamma_{s0}$. With this assumption, Eq. (D4) becomes

$$\gamma_{s0} = \frac{3}{2}(\gamma_s + v) \quad (\text{D5})$$

Parameter rescaling [req. (6)]. Finally, we require that the Schmidt number be invariant after rescaling: $\text{Sc} \equiv \nu/D_s = \gamma_{s0}/v_0 = \gamma_s/v$, which fixes the ratio of the rescaled collision frequencies to the ratio of their base values. Substituting $v = \gamma_s/\text{Sc}$ into Eq. (D5) and solving for γ_s leads to the condition

$$\gamma_s = \frac{2}{3} \frac{\text{Sc}}{\text{Sc} + 1} \gamma_{s0} = \left(\frac{a_0}{a} \right)^2 \gamma_{s0} \quad (\text{D6})$$

where the second equality is obtained by recalling that a is determined by preserving the long-time asymptotic form of the VACF [req. (6)], which implies

$$a^2 = \frac{3}{2} \left(1 + \text{Sc}^{-1} \right) a_0^2 \quad (\text{D7})$$

Thus, γ_s , v , and γ may be determined, respectively, via $\gamma_{s0} = v_0^2/D_s$, $v_0 = v_0^2/\nu$, and $\gamma_0 = v_0^2/\mu$ given known inputs for the transport coefficients (D_s , ν , and μ).

Parameters for gaseous and supercritical argon. Given the sparsity of numerical and experimental data for transport coefficients of dilute monatomic gases, the VACFs in Fig. 3 were produced using transport coefficients calculated from Enskog theory,^{11,149,150} supplemented by isothermal data for argon (at 130 K and 300 K) from the NIST Chemistry WebBook. For the transport coefficients, we took $D_s \rightarrow D_E = v_0^2/\gamma_{s0}$, $\nu \rightarrow \nu_E = v_0^2/v_0$, and $\mu \rightarrow \nu_{bE} = v_0^2/\gamma_0$, where

$$D_E \equiv 1.01896 \frac{D_0}{g(\sigma)} \quad (\text{D8})$$

$$\nu_E \equiv 1.016 \nu_0 \left[\frac{1}{g(\sigma)} + 0.8(bn_0) + 0.7615(bn_0)^2 g(\sigma) \right] \quad (\text{D9})$$

$$\nu_{bE} \equiv \frac{16}{5\pi} \nu_0 (bn_0)^2 g(\sigma) \quad (D10)$$

are the Enskog diffusion coefficient, (kinematic) shear viscosity, and (kinematic) bulk viscosity, respectively.¹⁵⁰

In Eqs. (D8) to (D10), n_0 is the equilibrium number density, σ the hard-sphere diameter, and $b \equiv (2/3)\pi\sigma^3$ is the second virial coefficient for a hard-sphere fluid. D_0 and ν_0 are the values of the self-diffusion and shear viscosity coefficients in the limit of zero density,

$$D_0 \equiv \frac{3v_0}{8\sqrt{\pi}n_0\sigma^2} \quad (D11)$$

$$\nu_0 \equiv \frac{5v_0}{16\sqrt{\pi}n_0\sigma^2} \quad (D12)$$

and $g(\sigma)$ is the radial distribution function evaluated at the hard-sphere point of contact. Analytic approximations for $g(\sigma)$ can be obtained from the Percus-Yevick equation, scaled particle theory,^{151–153} or the Carnahan-Starling equation of state;^{154–156} we used the Carnahan-Starling approximation for the 3D pair distribution:

$$g(\sigma) \approx \frac{1 - \phi/2}{(1 - \phi)^3} \quad (D13)$$

where the packing fraction $\phi \equiv (\pi/6)n_0\sigma^3$.

For all calculations in Fig. 3, we used a Gaussian static spectrum ($p = 2$) primarily as proof-of-principle, though one should expect higher values of p to apply only at the highest densities; e.g., in the liquid state, where propagating longitudinal and shear wave modes may be significant for softer intermolecular potentials. We also took $\sigma = 3.405 \text{ \AA}$ (argon Lennard-Jones diameter), $m = 40 \text{ Da}$ for the (atomic) mass, and set $\mathcal{D}_\perp = v_0^2/v$ (as discussed above) and $\mathcal{D}_\parallel = 4\mu/3$ (as in the liquid case). We determined v_\parallel^2 from the adiabatic index, i.e., $v_\parallel^2/v_0^2 = C_P/C_V$, using heat capacity values obtained from the NIST Chemistry WebBook for each combination of temperature and density, T and ρ_0 , where $\rho_0 = mn_0$.

Appendix E: Comparison with MD calculations for a supercritical Lennard-Jones fluid

In Ref. 28, MD simulations are performed for a supercritical Lennard-Jones (LJ) fluid at a reduced density $n_0^* = n_0\sigma^3 = 0.5$ and reduced temperature $T^* = k_B T/\epsilon = 1.5$, where σ and ϵ are the LJ diameter and energy, respectively. To compare with the results of Ref. 28, we took $m = 40 \text{ Da}$, $\sigma = 3.405 \text{ \AA}$, and $\epsilon = 120 \text{ K}$, [CITE] so that the (dimensional) mass density and temperature are, respectively, $\rho = mn_0 = 841.3 \text{ kg/m}^3$ and $T = 180 \text{ K}$; note that, for this temperature-density combination, $P \approx 19.2 \text{ MPa}$. For v_\parallel , we again use the adiabatic index computed from heat capacities obtained from the NIST Chemistry WebBook, SRD 69 for isothermal properties of argon (i.e., $v_\parallel^2/v_0^2 = C_P/C_V$). To obtain base values for the collision frequencies, i.e., v_0 ,

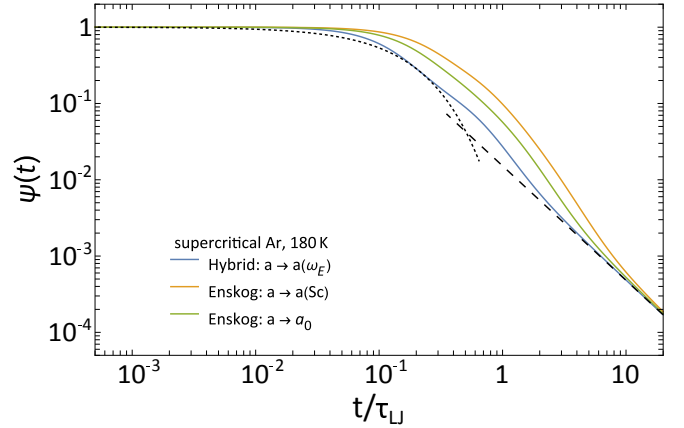


FIG. E.1. VACFs corresponding to a dense supercritical Lennard-Jones fluid studied in Ref. 28 (cf. Fig. 1). The VACF from the hybrid procedure described in this appendix (blue) is depicted with VACFs produced for two different (larger) values of a : setting $a \rightarrow \sqrt{(3/2)(1 + \text{Sc}^{-1})}a_0$ via Eq. (D7) (orange) and explicitly fixing $a \rightarrow a_0$ (green).

γ_0 , etc., we used the same Enskog diffusion and viscosity coefficient formulas given in Appendix D. However, we chose to treat this comparatively dense supercritical (SC) state slightly differently, as the packing fraction is $\phi \approx 0.262$ —more than half of argon’s triple point (TP) density ($\phi \approx 0.445$). In particular, we employed a hybrid treatment (detailed below) wherein the molecular scale a was computed via the second-moment condition [req. (5) and Eq. (B7)] using simple physical arguments to obtain an estimated Einstein frequency of $\omega_E = 4.75 \text{ ps}^{-1}$. The resulting VACF—Fig. E.1, blue—is in striking agreement with the MD calculations shown in Fig. 1 of Ref. 28. Our estimate for the Einstein frequency is based on the following calculations and physical reasoning.

First, at $\phi \approx 0.262$, the mean interparticle separation (center-to-center) is $d_0^{\text{SC}} \sim n_0^{-1/3} \approx 4.29 \text{ \AA}$, so the contact (surface-to-surface) distance, d^{SC} , may be estimated as $d^{\text{SC}} \approx d_0^{\text{SC}} - \sigma \approx 0.885 \text{ \AA}$; likewise, $d^{\text{TP}} \approx 0.190 \text{ \AA}$ at the TP. It is within reason to assume the Einstein frequency, ω_E , is physically relevant for SC argon at the given density because the surface-to-surface spacing is (still) substantially smaller than the particle diameter; i.e., we assume that particles cannot easily “break through the cage” formed by its neighbors at this (packing) density. Second, to arrive at an estimate for ω_E , we assume that the larger interparticle spacing in the SC case leads to an increased oscillation period, $\Delta\tau$, over that of TP argon, where $\Delta\tau = \tau^{\text{SC}} - \tau^{\text{TP}}$, and $\tau^{\text{SC}} \equiv 2\pi/\omega_E^{\text{SC}}$ and $\tau^{\text{TP}} \equiv 2\pi/\omega_E^{\text{TP}}$ are the respective oscillation periods. Finally, to estimate the increase in oscillation period, we make the simple physical assumption that $\Delta\tau$ is an intervening *ballistic* interval arising from the increased surface-to-surface distance, an additional separation of $d^{\text{SC}} - d^{\text{TP}} \approx 0.695 \text{ \AA}$ over the TP case. This leads to $\Delta\tau \approx 2(d^{\text{SC}} - d^{\text{TP}})/v_b$, where the factor of 2 accounts for two ballistic traversals per cage oscillation and we

take the ballistic speed to $v_b \approx \sqrt{2k_B T/m} = \sqrt{2}v_0$ (i.e., the most probable speed of a Maxwell-Boltzmann distribution).

Putting everything together, we arrive at a rough estimate for the oscillation period for the dense SC fluid:

$$\begin{aligned}\tau^{\text{SC}} &= \frac{2\pi}{\omega_E^{\text{TP}}} + \frac{2(d^{\text{SC}} - d^{\text{TP}})}{\sqrt{2}v_0^2} \\ &\approx \frac{2\pi}{7.7 \text{ ps}^{-1}} + \frac{20.695 \text{ \AA}}{2.74 \text{ \AA}/\text{ps}} \\ &\approx 1.32 \text{ ps}\end{aligned}$$

which yields for the Einstein frequency

$$\omega_E^{\text{SC}} = \frac{2\pi}{\tau^{\text{SC}}} \approx 4.75 \text{ ps}^{-1} \quad (\text{E1})$$

Finally, we use a generalized Gaussian spectrum with $p \approx 1.5$ for which Eq. (B7) gives $a \approx 2.28 \text{ \AA}$ and yields excellent agreement (Fig. E.1, blue) throughout the timescales sampled by MD. Note that time is expressed in LJ reduced units, $t^* \equiv t/\tau_{\text{LJ}}$, where $\tau_{\text{LJ}} \equiv \sqrt{m\sigma^2/\epsilon}$ is the characteristic LJ timescale; for argon, $\tau_{\text{LJ}} \approx 2.156 \text{ ps}$. Figure E.1 also shows VACFs computed using two different (larger) values of a : computing a from Eq. (D7) for dilute fluids (orange) and explicitly setting $a \rightarrow a_0$ (green). Note that the blue curve reproduces the rather subtle “plateau” region ($t^* \approx 0.15\text{--}0.6$) due to the sound-like mode originating from the longitudinal component, as well as the nuanced transition from exponential-like to diffusive decay for $t^* \gtrsim 1$.

REFERENCES

- ¹J. P. Boon and S. Yip, *Molecular Hydrodynamics* (Dover, New York, 1991).
- ²D. A. McQuarrie, *Statistical Mechanics*, 1st ed. (University Science Books, Sausalito, 2000).
- ³J.-P. Hansen and I. R. McDonald, *Theory of Simple Liquids: with Applications to Soft Matter*, 4th ed. (Academic Press, Oxford, 2013).
- ⁴A. Einstein, *Ann. Phys.* **322**, 549 (1905).
- ⁵B. J. Alder and T. E. Wainwright, *Phys. Rev. Lett.* **18**, 988 (1967).
- ⁶B. J. Alder and T. E. Wainwright, *Phys. Rev. A* **1**, 18 (1970).
- ⁷D. Enskog, Uppsala: Almquist & Wiksells Boktryckeri (1917).
- ⁸D. Enskog, *Vetenskaps Akad. Handl.* **63** (1922).
- ⁹S. G. Brush, *Kinetic Theory: The Chapman-Enskog solution of the transport equation for moderately dense gases*, Vol. 3 (Pergamon Press, Oxford, 1972).
- ¹⁰P. M. V. Resibois and M. De Leener, *Classical kinetic theory of fluids*, 1st ed. (Wiley, New York, 1977).
- ¹¹S. Chapman and T. G. Cowling, *The Mathematical Theory of Non-uniform Gases: An Account of the Kinetic Theory of Viscosity, Thermal Conduction and Diffusion in Gases*, 3rd ed. (Cambridge University Press, Cambridge, 1990).
- ¹²R. Zwanzig and M. Bixon, *Phys. Rev. A* **2**, 2005 (1970).
- ¹³P. Schofield, in *Statistical Mechanics*, SPR - Statistical Mechanics, Vol. 2, edited by K. Singer (The Royal Society of Chemistry, 1975) pp. 1–54.
- ¹⁴P. C. Martin and S. Yip, *Phys. Rev.* **170**, 151 (1968).
- ¹⁵D. Forster, P. C. Martin, and S. Yip, *Phys. Rev.* **170**, 155 (1968).
- ¹⁶K. Kim and M. Nelkin, *Phys. Rev. A* **4**, 2065 (1971).
- ¹⁷Y. Pomeau and P. Résibois, *Phys. Rep.* **19**, 63 (1975).
- ¹⁸R. W. Zwanzig, *Lectures in Theoretical Physics*, edited by W. E. Brittin, B. W. Downs, and J. Downs, Lectures Delivered at the Summer Institute for Theoretical Physics, Vol. 3 (Wiley Interscience, New York, 1961) pp. 106–141.
- ¹⁹H. Mori, *Progr. Theoret. Phys.* **33**, 423 (1965).
- ²⁰H. Mori, *Progr. Theoret. Phys.* **34**, 399 (1965).
- ²¹D. Levesque and L. Verlet, *Phys. Rev. A* **2**, 2514 (1970).
- ²²D. Levesque, L. Verlet, and J. Kürkijarvi, *Phys. Rev. A Gen. Phys.* **7**, 1690 (1973).
- ²³J. Kushick and B. J. Berne, *J. Chem. Phys.* **59**, 3732 (1973).
- ²⁴P. Schofield, *Comput. Phys. Commun.* **5**, 17 (1973).
- ²⁵I. M. de Schepper, J. C. van Rijs, A. A. van Well, P. Verkerk, L. A. de Graaf, and C. Bruin, *Phys. Rev. A* **29**, 1602 (1984).
- ²⁶A. McDonough, S. P. Russo, and I. K. Snook, *Phys. Rev. E Stat. Nonlin. Soft Matter Phys.* **63**, 026109 (2001).
- ²⁷R. F. A. Dib, F. Ould-Kaddour, and D. Levesque, *Phys. Rev. E Stat. Nonlin. Soft Matter Phys.* **74**, 011202 (2006).
- ²⁸D. Lesnicki, R. Vuilleumier, A. Carof, and B. Rotenberg, *Phys. Rev. Lett.* **116**, 147804 (2016).
- ²⁹T. Sanghi, R. Bhaduria, and N. R. Aluru, *J. Chem. Phys.* **145**, 134108 (2016).
- ³⁰K. H. Han, C. Kim, P. Talkner, G. E. Karniadakis, and E. K. Lee, *J. Chem. Phys.* **148**, 024506 (2018).
- ³¹K. Mizuta, Y. Ishii, K. Kim, and N. Matubayasi, *Soft Matter* **15**, 4380 (2019).
- ³²H. Zhao and H. Zhao, *Phys Rev E* **103**, L030103 (2021).
- ³³Z. Li, X. Bian, X. Li, and G. E. Karniadakis, *J. Chem. Phys.* **143**, 243128 (2015).
- ³⁴P. Español and A. Donev, *J. Chem. Phys.* **143**, 234104 (2015).
- ³⁵G. Jung and F. Schmid, *J. Chem. Phys.* **144**, 204104 (2016).
- ³⁶G. Jung, M. Hanke, and F. Schmid, *J. Chem. Theory Comput.* **13**, 2481 (2017).
- ³⁷G. Jung and F. Schmid, *Phys. Fluids* **29**, 126101 (2017).
- ³⁸V. Klippenstein, M. Tripathy, G. Jung, F. Schmid, and N. F. A. van der Vegt, *J. Phys. Chem. B* [10.1021/acs.jpcb.1c01120](https://doi.org/10.1021/acs.jpcb.1c01120) (2021).
- ³⁹J. T. Padding and A. A. Louis, *Phys. Rev. E Stat. Nonlin. Soft Matter Phys.* **74**, 031402 (2006).
- ⁴⁰L. Wang and M. Quintard, in *Advances in Transport Phenomena: 2009*, edited by L. Wang (Springer Berlin Heidelberg, Berlin, Heidelberg, 2009) pp. 179–243.
- ⁴¹G. Jung, M. Hanke, and F. Schmid, *Soft Matter* **14**, 9368 (2018).
- ⁴²D. L. Koch and G. Subramanian, *Annu. Rev. Fluid Mech.* **43**, 637 (2011).
- ⁴³S. Wang and A. M. Ardekani, *J. Fluid Mech.* **702**, 286 (2012).
- ⁴⁴J. Elgeti, R. G. Winkler, and G. Gompper, *Rep. Prog. Phys.* **78**, 056601 (2015).
- ⁴⁵J. García De La Torre, M. L. Huertas, and B. Carrasco, *Biophys. J.* **78**, 719 (2000).
- ⁴⁶M. X. Fernandes and J. G. de la Torre, *Biophys. J.* **83**, 3039 (2002).
- ⁴⁷C. P. Brangwynne, G. H. Koenderink, F. C. MacKintosh, and D. A. Weitz, *J. Cell Biol.* **183**, 583 (2008).
- ⁴⁸R. Kapral and A. S. Mikhailov, *Physica D* **318-319**, 100 (2016).
- ⁴⁹J. R. Howse, R. A. L. Jones, A. J. Ryan, T. Gough, R. Vafabakhsh, and R. Golestanian, *Phys. Rev. Lett.* **99**, 048102 (2007).
- ⁵⁰M.-J. Huang, J. Schofield, P. Gaspard, and R. Kapral, *J. Chem. Phys.* **149**, 024904 (2018).
- ⁵¹P. Gaspard and R. Kapral, *J. Chem. Phys.* **148**, 134104 (2018).
- ⁵²G. Szamel, *J. Chem. Phys.* **150**, 124901 (2019).
- ⁵³F. B. Usabiaga, X. Xie, R. Delgado-Buscalioni, and A. Donev, *J. Chem. Phys.* **139**, 214113 (2013).
- ⁵⁴M. H. Ernst, E. H. Hauge, and J. M. J. van Leeuwen, *Phys. Rev. Lett.* **25**, 1254 (1970).
- ⁵⁵M. H. Ernst, E. H. Hauge, and J. M. J. van Leeuwen, *Phys. Rev. A* **4**, 2055 (1971).
- ⁵⁶T. Gaskell and S. Miller, *J. phys.* **11**, 3749 (1978).

⁵⁷T. Gaskell and S. Miller, *J. phys.* **11**, 4839 (1978).

⁵⁸T. Gaskell and S. Miller, *J. phys.* **12**, 2705 (1979).

⁵⁹H. Grad, *Communications on pure and applied mathematics* **2**, 331 (1949).

⁶⁰H. Struchtrup and M. Torrilhon, *Phys. Fluids* **15**, 2668 (2003).

⁶¹H. C. Öttinger, *Beyond Equilibrium Thermodynamics*, edited by H. C. Öttinger (John Wiley & Sons, 2005).

⁶²H. Öttinger and H. Struchtrup, *Multiscale Model. Simul.* **6**, 53 (2007).

⁶³D. Jou, J. Casas-Vázquez, and M. Criado-Sancho, *Thermodynamics of Fluids Under Flow* (Springer Science & Business Media, 2010).

⁶⁴H. C. Öttinger, *Phys. Rev. Lett.* **104**, 120601 (2010).

⁶⁵H. Struchtrup and M. Torrilhon, *Phys. Fluids* **25**, 052001 (2013).

⁶⁶M. Torrilhon, *Commun. Comput. Phys.* **18**, 529 (2015).

⁶⁷P. L. Bhatnagar, E. P. Gross, and M. Krook, *Phys. Rev.* **94**, 511 (1954).

⁶⁸R. Zwanzig, *Nonequilibrium Statistical Mechanics* (Oxford University Press, Oxford, 2001).

⁶⁹Y. L. Klimontovich, *Statistical Theory of Open Systems: Volume 1: A Unified Approach to Kinetic Description of Processes in Active Systems*, edited by A. Van Der Merwe, *Fundamental Theories of Physics*, Vol. 67 (Kluwer Academic Publishers, Dordrecht, 2012).

⁷⁰R. Zwanzig and R. D. Mountain, *J. Chem. Phys.* **43**, 4464 (1965).

⁷¹P. Schofield, *Proc. Phys. Soc. London* **88**, 149 (1966).

⁷²B. J. Alder and W. E. Alley, *Phys. Today* **37**, 56 (1984).

⁷³C.-H. Chung and S. Yip, *Phys. Rev.* **182**, 323 (1969).

⁷⁴U. Balucani, R. Vallauri, T. Gaskell, and M. Gori, *J. Phys. C: Solid State Phys.* **18**, 3133 (1985).

⁷⁵U. Balucani, R. Vallauri, and T. Gaskell, *Phys. Rev. A Gen. Phys.* **35**, 4263 (1987).

⁷⁶T. Gaskell and M. S. Woolfson, *J. Phys. C: Solid State Phys.* **15**, 6339 (1982).

⁷⁷U. Balucani, R. Vallauri, and T. Gaskell, *Ber. Bunsenges. Phys. Chem.* **94**, 261 (1990).

⁷⁸N. Anento, J. A. Padró, and M. Canales, *J. Chem. Phys.* **111**, 10210 (1999).

⁷⁹M. Colangeli, M. Kröger, and H. C. Öttinger, *Phys. Rev. E Stat. Nonlin. Soft Matter Phys.* **80**, 051202 (2009).

⁸⁰G. Garberoglio, R. Vallauri, and U. Bafile, *J. Chem. Phys.* **148**, 174501 (2018).

⁸¹U. Balucani, R. Vallauri, T. Gaskell, and M. Gori, *Phys. Lett. A* **102**, 109 (1984).

⁸²D. C. Leslie, *Rep. Prog. Phys.* **36**, 1365 (1973).

⁸³V. S. L'vov, *Scale invariant theory of fully developed hydrodynamic turbulence-Hamiltonian approach* (1991).

⁸⁴Y. Zhou, *Phys. Rep.* **935**, 1 (2021).

⁸⁵A. Z. Akcasu and E. Daniels, *Phys. Rev. A Gen. Phys.* **2**, 962 (1970).

⁸⁶S.-H. Chen and A. Rahman, *Mol. Phys.* **34**, 1247 (1977).

⁸⁷G. Karniadakis, A. Beskok, and N. Aluru, *Microflows and Nanoflows: Fundamentals and Simulation*, edited by S. S. Antman, J. E. Marsden, and L. Sirovich, *Interdisciplinary Applied Mathematics*, Vol. 29 (Springer, New York, 2005).

⁸⁸S. L. Seyler, *Computational Approaches to Simulation and Analysis of Large Conformational Transitions in Proteins*, Ph.D. thesis, Arizona State University (2017).

⁸⁹H. Van Beijeren and M. H. Ernst, *Physica* **68**, 437 (1973).

⁹⁰H. Van Beijeren and M. H. Ernst, *Physica* **70**, 225 (1973).

⁹¹J. Karkheck and G. Stell, *J. Chem. Phys.* **75**, 1475 (1981).

⁹²D. Henderson, *Fundamentals of Inhomogeneous Fluids* (CRC Press, New York, 1992).

⁹³D. Schiff, *Phys. Rev.* **186**, 151 (1969).

⁹⁴T. Geszti, *J. Phys. C: Solid State Phys.* **9**, L263 (1976).

⁹⁵A. Rahman, *Phys. Rev. A* **9**, 1667 (1974).

⁹⁶E. N. D. C. Andrade and E. R. Dobbs, *Proc. R. Soc. Lond. A Math. Phys. Sci.* **211**, 12 (1952).

⁹⁷E. W. Lemmon and R. T. Jacobsen, *Int. J. Thermophys.* **25**, 21 (2004).

⁹⁸A. H. M. Zaheri, S. Srivastava, and K. Tankeshwar, *J. Phys. Condens. Matter* **15**, 6683 (2003).

⁹⁹R. S. Chatwell and J. Vrabec, *J. Chem. Phys.* **152**, 094503 (2020).

¹⁰⁰J. J. Van Loef, *Physica* **75**, 115 (1974).

¹⁰¹D. Fincham and D. M. Heyes, *Chem. Phys.* **78**, 425 (1983).

¹⁰²M. H. Ernst, E. H. Hauge, and J. M. J. van Leeuwen, *Phys. Lett. A* **34**, 419 (1971).

¹⁰³J. R. Dorfman and E. G. D. Cohen, *Phys. Rev. Lett.* **25**, 1257 (1970).

¹⁰⁴J. R. Dorfman and E. G. D. Cohen, *Phys. Rev. A* **12**, 292 (1975).

¹⁰⁵U. Balucani, A. Torcini, and R. Vallauri, *Phys. Rev. A* **46**, 2159 (1992).

¹⁰⁶F. B. Usabiaga, I. Pagonabarraga, and R. Delgado-Buscalioni, *J. Comput. Phys.* **235**, 701 (2013).

¹⁰⁷F. Balboa Usabiaga, R. Delgado-Buscalioni, B. E. Griffith, and A. Donev, *Comput. Methods Appl. Mech. Eng.* **269**, 139 (2014).

¹⁰⁸J. V. Boussinesq, *C. R. Acad. Sci. Paris* **100**, 935 (1885).

¹⁰⁹A. B. Basset, *Proc. Lond. Math. Soc.* **s1-19**, 46 (1887).

¹¹⁰C. W. Oseen, *Neuere methoden und ergebnisse in der hydrodynamik* (1927).

¹¹¹M. R. Maxey and J. J. Riley, *Phys. Fluids* **26**, 883 (1983).

¹¹²P. Gaspard, *Physica A: Statistical Mechanics and its Applications*, 121823 (2019).

¹¹³S. L. Seyler and Pressé, Steve, *Phys. Rev. Research* **1**, 032003 (2019).

¹¹⁴K. Trachenko, *Phys Rev E* **96**, 062134 (2017).

¹¹⁵R. Fürth, *Ann. Phys.* **53**, 177 (1917).

¹¹⁶G. I. Taylor, *Proc. Lond. Math. Soc.* **2**, 196 (1922).

¹¹⁷S. Goldstein, *Quart. J. Mech. Appl. Math.* **4**, 129 (1951).

¹¹⁸S. A. Khrapak, *Molecules* **26**, 10.3390/molecules26247499 (2021).

¹¹⁹R. Zwanzig, *J. Chem. Phys.* **79**, 4507 (1983).

¹²⁰D. Lesnicki and R. Vuilleumier, *J. Chem. Phys.* **147**, 094502 (2017).

¹²¹L. D. Landau and E. M. Lifshitz, *Fluid Mechanics*, 3rd ed., Vol. 6 (Pergamon Press, Oxford, 1966).

¹²²U. Balucani and M. Zoppi, *Dynamics of the Liquid State*, edited by S. W. Lovesey and E. W. J. Mitchell, *Oxford Series on Neutron Scattering in Condensed Matter*, Vol. 10 (Clarendon Press, Oxford, 1994).

¹²³T. S. Chow and J. J. Hermans, *J. Chem. Phys.* **56**, 3150 (1972).

¹²⁴M. Nelkin, *The Physics of Fluids* **15**, 1685 (1972).

¹²⁵S. L. Seyler and Pressé, *J. Chem. Phys.* **153**, 041102 (2020).

¹²⁶D. Chakraborty, *Eur. Phys. J. B* **83**, 375 (2011).

¹²⁷J. Lee, S. L. Seyler, and Pressé, *J. Chem. Phys.* **151**, 094108 (2019).

¹²⁸I. Goychuk, *Phys. Rev. Lett.* **123**, 180603 (2019).

¹²⁹I. Goychuk and T. Pöschel, *Phys. Rev. E* **102**, 012139 (2020).

¹³⁰M. V. Díaz, *Eur. Phys. J. E Soft Matter* **44**, 141 (2021).

¹³¹B. J. Cherayil, *J. Phys. Chem. B* **10.1021/acs.jpcb.2c03273** (2022).

¹³²J. Spiechowicz, I. G. Marchenko, P. Hänggi, and J. Luczka, *Entropy* **25**, 10.3390/e25010042 (2022).

¹³³G. Pastore, B. Bernu, J. P. Hansen, and Y. Hiwatari, *Phys. Rev. A Gen. Phys.* **38**, 454 (1988).

¹³⁴U. Balucani, R. Vallauri, and T. Gaskell, *Nuovo Cimento C* **12**, 511 (1990).

¹³⁵G. Ren and Y. Wang, *Phys. Chem. Chem. Phys.* **23**, 24541 (2021).

¹³⁶V. A. Levashov, J. R. Morris, and T. Egami, *J. Chem. Phys.* **138**, 044507 (2013).

¹³⁷U. R. Pedersen, N. P. Bailey, T. B. Schrøder, and J. C. Dyre, *Phys. Rev. Lett.* **100**, 015701 (2008).

¹³⁸N. Ohtori, S. Miyamoto, and Y. Ishii, *Phys Rev E* **95**, 052122 (2017).

¹³⁹Y. D. Fomin, V. N. Ryzhov, E. N. Tsiok, J. E. Proctor, C. Prescher, V. B. Prakapenka, K. Trachenko, and V. V. Brazhkin, *J. Phys. Condens. Matter* **30**, 134003 (2018).

¹⁴⁰F. Lantelme, P. Turq, and P. Schofield, *J. Chem. Phys.* **71**, 2507 (1979).

¹⁴¹R. Malik, D. Burch, M. Bazant, and G. Ceder, *Nano Lett.* **10**, 4123 (2010).

¹⁴²J. P. de Souza and M. Z. Bazant, *J. Phys. Chem. C* **124**, 11414 (2020).

¹⁴³P. K. Ghorai and D. V. Matyushov, *J. Phys. Chem. B* **124**, 3754 (2020).

¹⁴⁴S. M. Sarhangi and D. V. Matyushov, *J. Phys. Chem. Lett.* , 10137 (2020).

¹⁴⁵T. Samanta and D. V. Matyushov, *Phys. Rev. Research* **3**, 023025 (2021).

¹⁴⁶K. Meier, A. Laesecke, and S. Kabelac, *J. Chem. Phys.* **122**, 14513 (2005).

¹⁴⁷F. Jaeger, O. K. Matar, and E. A. Müller, *J. Chem. Phys.* **148**, 174504 (2018).

¹⁴⁸B. Sharma, S. Pareek, and R. Kumar, *Eur. J. Mech. B. Fluids* **98**, 32 (2023).

¹⁴⁹J. J. Erpenbeck and W. W. Wood, *Phys. Rev. A* **43**, 4254 (1991).

¹⁵⁰D. M. Heyes, S. Pieprzyk, and A. C. Brańka, *J. Chem. Phys.* **157**, 114502 (2022).

¹⁵¹H. Reiss, H. L. Frisch, and J. L. Lebowitz, *J. Chem. Phys.* **31**, 369 (1959).

¹⁵²H. Reiss, H. L. Frisch, E. Helfand, and J. L. Lebowitz, *J. Chem. Phys.* **32**, 119 (1960).

¹⁵³E. Helfand, H. Reiss, H. L. Frisch, and J. L. Lebowitz, *J. Chem. Phys.* **33**, 1379 (1960).

¹⁵⁴N. F. Carnahan and K. E. Starling, *J. Chem. Phys.* **51**, 635 (1969).

¹⁵⁵Y. Song, E. A. Mason, and R. M. Stratt, *J. Phys. Chem.* **93**, 6916 (1989).

¹⁵⁶H. Sigurgeirsson and D. M. Heyes, *Mol. Phys.* **101**, 469 (2003).